Everything You Ever Wanted to Know About Frequency-Selective Surface Filters but Were Afraid to Ask

Benjamin Hooberman

May 2005

Contents

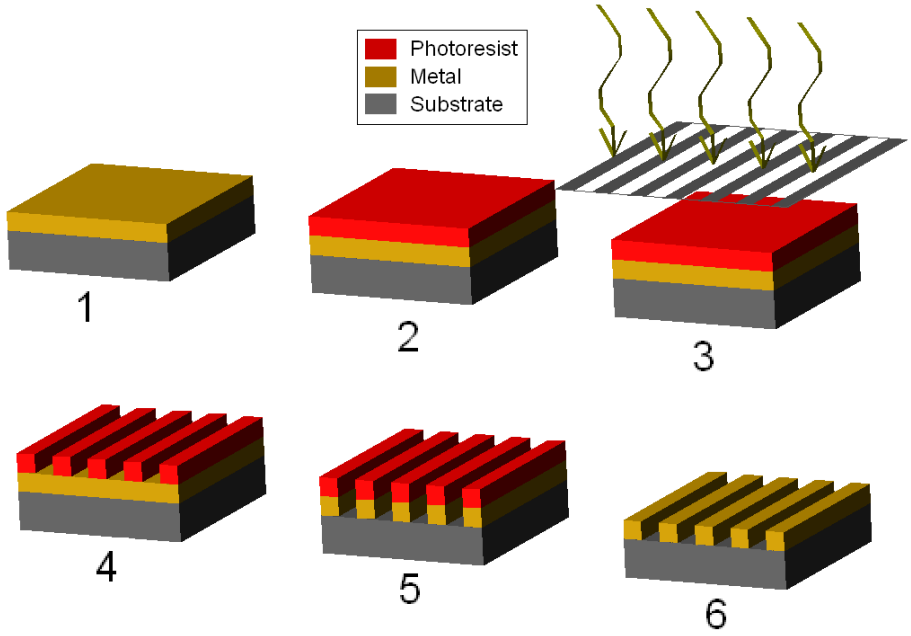

Figure 1: Step-by-step photolithography process used to produce FSS filters.

1 Abstract

In this paper we discuss the theory of frequency-selective surface (FSS) filters. FSS filters consist of metallic grids deposited on a polymer substrate and have applications in bolometer-based CMB experiments. We begin by reviewing the photolithography process used to produce the filters. Next we explain the physical mechanism on which the filters function: induced electron oscillations driven by a source E-field. We review the equivalent circuit transmission line theory and use matrix methods to analyze these circuits and obtain reflectance and transmittance data.

2 Production

The photolithography process used to produce the filters is shown in figure 1. We begin by evaporating a thin metal film onto a substrate. Next, we spread a film of photoresist onto the sample and place it in a mask aligner. In the mask aligner, UV light passes through a glass mask and strikes the sample. The sample is placed in developer, which removes the photoresist that has been exposed to UV. We then place the sample in a chemical bath which etches the metal film under the photoresist. Finally, we wash off the remaining photoresist with a stripper and clean the sample with methanol and de-ionized water.

2.1 Evaporation of Metal Film

The substrate (either polyethylene or polypropylene) is placed in an evaporator which deposits a thin film of metal (either copper or aluminum) onto the sample. This metal film, which will be etched to form our desired pattern, is extremely uniform and has thickness on the order of hundreds of nanometers.

2.2 Application of Photoresist

The sample, now consisting of a metal film on a polymer substrate, is placed on a spinner. Photoresist is applied and the sample is spun at high speed, resulting in a uniform thin film of photoresist on the sample surface.

2.3 Mask Exposure

After the photoresist has been placed in an oven and baked, the sample is placed in a mask aligner. A mask of ink on transparency or metal on glass is placed flush against the sample which is then exposed to UV light. The light can penetrate the glass only in the places where no ink is present, exposing the photoresist to UV in these places.

2.4 Developing the Photoresist

The sample is placed in a developer solution, which washes away the photoresist in the places where it has been exposed to UV. The rest of the photoresist remains to protect the metal film from the etchant.

2.5 Etching

The sample is placed in a metal etchant solution. The etchant can only reach the metal that is not covered by photoresist; this metal is removed and the rest remains. At this point the pattern on the mask has been etched into the metal film.

2.6 Photoresist Removal and Cleaning

Finally, the remaining photoresist is removed by placing the sample in a stripper solution. The sample is cleaned thoroughly with methanol and de-ionized water.

3 Review of Relevant Concepts

Before proceeding to a detailed analysis of FSS filters we begin by reviewing the relevant concepts in electromagnetic theory. This will allow us to understand the underlying mechanism on which the filters function.

In figure 2a we see a plane wave source incident from the left which strikes a metal plane at normal incidence. Let us imagine that a single electron sits in the plane and try to understand what happens when the wave strikes the filter. Because the plane is orthogonal to the Poynting vector, the E-vector of the source lies in the plane. This E-vector exerts a force on the electron and causes it to oscillate. A portion of the energy from the source must therefore be

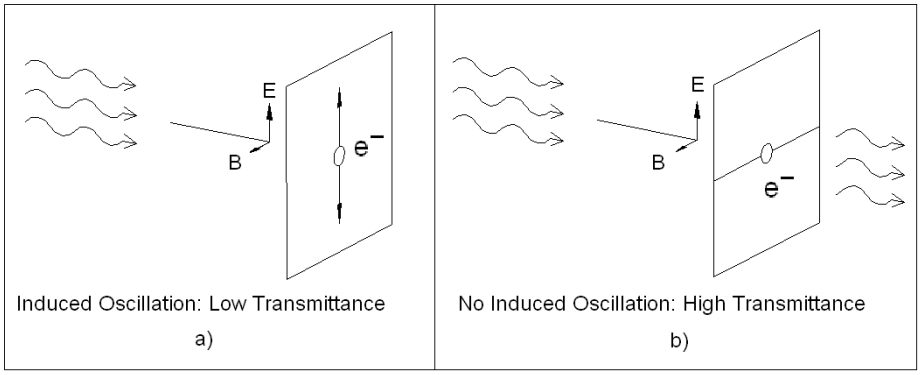

Figure 2: Electron in filter plane undergoes oscillations driven by source wave (left). Electron constrained to move along wire cannot undergo oscillations (right).

converted into kinetic energy in order for the electron to remain in the oscillating state. To preserve conservation of energy, only a fraction of the incident power will be transmitted and the rest is absorbed by the electron. If all of the energy from the wave is transferred to electrons in the metal, then the transmittance through the filter will be zero.

Let us now imagine a slightly different scenario. Imagine that we have a wire which lies in the metal plane but it also orthogonal to the E-vector of the incident plane wave as shown in figure 2b. If an electron is constrained to move along this wire, it will not absorb kinetic energy from the source because it is not allowed to accelerate in the direction that the force is exerted. In this case, the electron is effectively "invisible" to the incoming wave which will be fully transmitted.

To reiterate, when the electron does not absorb energy the wave is transmitted, when the electron absorbs energy the wave is not transmitted. But what happens to the incident wave energy which is not transmitted? As mentioned above, this energy is converted into kinetic energy, causing the electron to oscillate. But an oscillating electron will itself radiate as an electric dipole. This radiation is concentrated in the plane orthogonal to the oscillation axis, and the electron will therefore emit radiation on both sides of the filter. The key here is that the radiation emitted toward the right hand side of the diagram destructively interferes with the incident wave propagating from the left, resulting in a cancellation of the E-field on the right side of the filter. The dipole radiation emitted toward the left is what we refer to as the reflected wave.

This is the basic mechanism on which the filter functions. An incident plane wave strikes the filter and causes the electrons in the metal to oscillate. If a large portion of the incident energy is absorbed by these electrons they re-radiate and cancel the initial field, causing the transmittance through the filter to be low. In this case, the electrons will re-radiate toward the left and cause the reflected wave amplitude to be high. If only a small portion of the incident power is absorbed no such cancellation occurs and the transmittance will

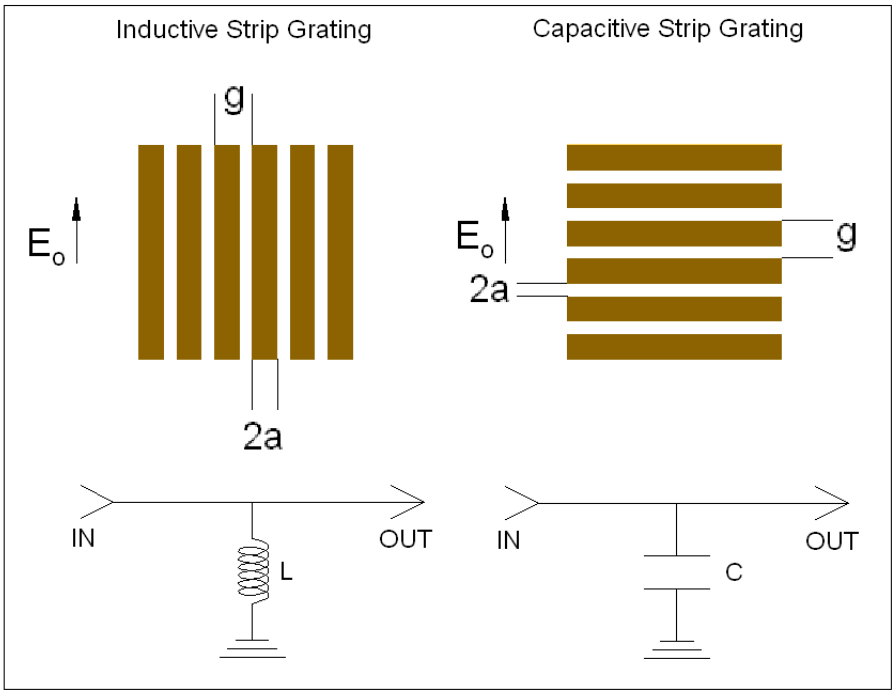

Figure 3: Layout of strip-grating filters.

be high. In general the transmittance through the filter is a function of frequency; in other words, the electrons in the metal will absorb and re-radiate some wavelengths with higher efficiency than others. The shape of the transmittance curve depends on the pattern etched into the metal filter, and we can etch various patterns into our metal to obtain filters of varying behavior.

4 Filter Geometries and Equivalent Circuits

The three most common classes of filters are strip grating filters, mesh filters, and cross-mesh filters. The strip grating filter is useful in illustrating the basic concepts needed to understand more complicated filter geometries, and we therefore begin our discussion with this type of filter. We continue to discuss mesh filters, which are useful because of their polarization-independence property. Finally, we discuss cross-mesh filters which can be used as band-pass and band-stop filters. The filter that we are most interested in is the inductive cross mesh filter which behaves as a bandpass filter.

4.1 Strip Grating Filters

The geometry of the strip grating filter is shown in figure 3. If the E-field is parallel to the metal strips we have an inductive strip-grating filter; if the E-field is perpendicular to the strips we have a capacitive strip-grating filter.

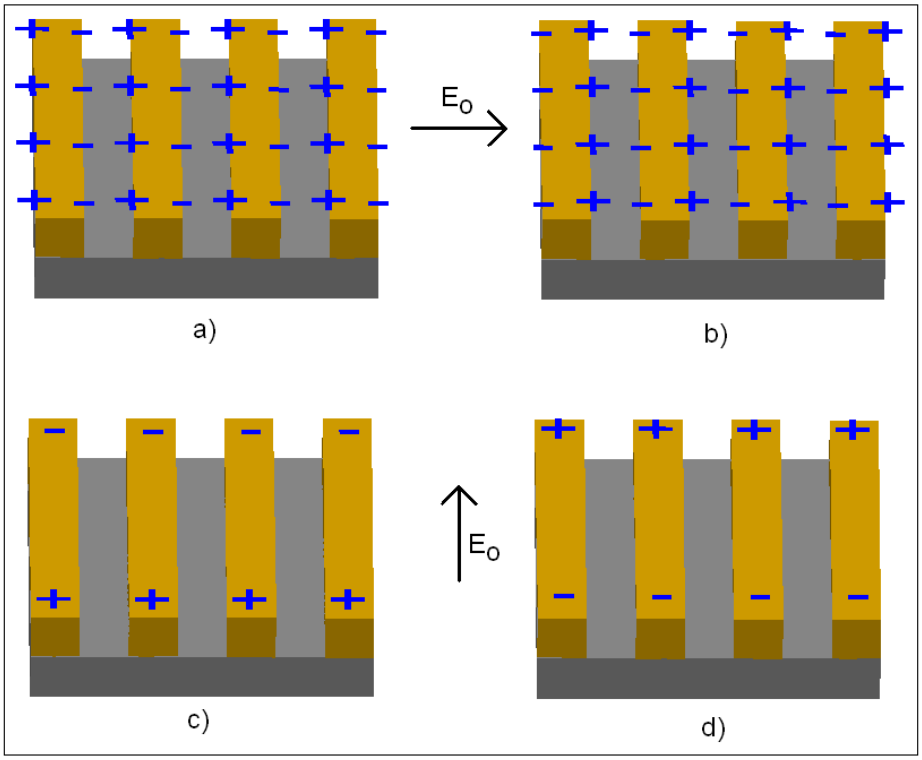

Figure 4: Arrangement of charge on strip grating filter. If the E-field is perpendicular to the strips the filter switches between states a and b, if it is parallel to the strip the filter switches between c and d.

We begin by examining the capacitive filter in which the electric field vector is perpendicular to the strips. The E-vector undergoes sinusoidal oscillations which induce the electrons in the metal to oscillate in the same direction (see figure 4). The filter will switch between the two states a and b as the electrons in the metal are driven back and forth.

We can guess what kind of behavior this filter will exhibit by examining two limiting cases: a monochromatic source of very low frequency (long wavelength compared to the grid spacing) and another monochromatic source of very high frequency (short wavelength compared to the grid spacing). First let's consider the long-wavelength limit. Imagine that such a source strikes a strip filter which is initially in the neutral state, driving it to one of the two charged states. The filter will remain in that state until the E-vector has time to reverse directions and drive the current in the opposite direction. However, since the E-vector of a long-wavelength source varies slowly, the electrons in the metal remain stationary for large periods of time and do not absorb energy during these periods. Therefore, only a small portion of the energy in the wave will be absorbed by the electrons and the transmittance will be high.

Next, consider the short-wavelength (high frequency) limit. When such a source strikes a filter initially in the neutral state, it will again drive the filter into one of the two charged states. This time, however, the filter will not remain in one state but will switch rapidly between the two due to the rapid oscillation of the E-field of the source. This means that the electrons in the metal are constantly oscillating and must therefore be absorbing energy from the incident wave. Therefore, a large portion of the incident wave energy will be absorbed and the transmittance will be low.

The above argument correctly predicts the transmittance of a capacitve strip grating filter. This is a "low-pass filter," since it will transmit low-frequency sources and reject higher frequencies. Notice that the arrangement of charge on the surface resembles that of a capacitor, suggesting that it may be possible to model the strip grating filter as a capacitive circuit element. Consider the circuit shown in figure 3 in which a capacitor shunts a transmission line to ground. In the configuration shown, a high-frequency source will drive a current across the capacitor and travel to ground. A high-frequency wave entering at the input of the transmission line will therefore not reach the output port. A low-frequency source will fail to drive a current across the capacitor and will therefore reach the output port. The equivalent circuit therefore behaves as a low-pass filter by shunting high-frequency sources to ground but allowing low-frequencies to pass. This is precisely how the capacitive strip-grating filter behaves, and we therefore refer to the circuit as the equivalent circuit corresponding to the capacitive strip geometry. As will be discussed in section 5, equivalent circuits are useful in analyzing the corresponding filter geometry.

Now consider the inductive strip grating filter in which the E-field of the source is parallel to the strips. Returning to our hypothetical limiting cases, imagine what will happen when a low-frequency (long-wavelength) source strikes the filter. The electrons residing in the metal are now free to move along the strips and will continue to move in the same direction until the E-field reverses directions. This time, however, the electrons are free to continue moving in the same direction for large periods of time because they move along the long dimension of the strips. In this case, the longer the wavelength of the source the longer the electrons can continue moving without changing direction. We

therefore expect a large amount of energy to be absorbed by the electrons, leading to low transmittance for a long-wavelength source.

Now for the high-frequency limit. The rapidly oscillating electric field of the incident wave will cause the electrons to oscillate. This time, however, the electrons move only a short distance before they must change directions. The electrons "wiggle" back and forth at high frequency but fail to exhibit the long-range motion excited by the long-wavelength source. This requires the absorption of only a small amount of power, and a high-frequency source will therefore have a high transmittance.

Again, we have correctly predicted the transmittance of the inductive strip grating filter, which does indeed function as a high-pass filter. The equivalent circuit corresponding to this filter geometry is an inductor which acts as a shunt to ground. A low-frequency source drives a current across the inductor and travels to ground, while a high-frequency source will not drive a current and will reach the output port. The shunt inductor therefore behaves as a high-pass filter as required.

As will be discussed in section 5, we are interested in the reactance of the equivalent circuit. The reactances of the capacitive and inductive strip grating filters were determined empirically to be [8]:

$$X(f)_{ind} = \frac{gf}{c} \ln \csc \frac{\pi a}{g} \tag{1}$$

$$X(f)_{cap} = \frac{-2}{n_1^2 + n_2^2} (\frac{4gf}{c} \ln \csc \frac{\pi a}{g})^{-1} \tag{2}$$

The major disadvantage of the strip grating filter geometry is that the transmittance depends on the polarization of the source. This is obvious, since the only difference between the capacitive and inductive strip grating filters is that the polarization vector is rotated through 90 degrees. This means that if we wish to use strip grating filters as high- or low-pass filters our source must be linearly polarized and aligned with one of the grid axes. If we wish to analyze un-polarized or partially polarized sources we must therefore use a different filter geometry. In the next section we review mesh filter geometries which do not suffer from this polarization-dependence problem.

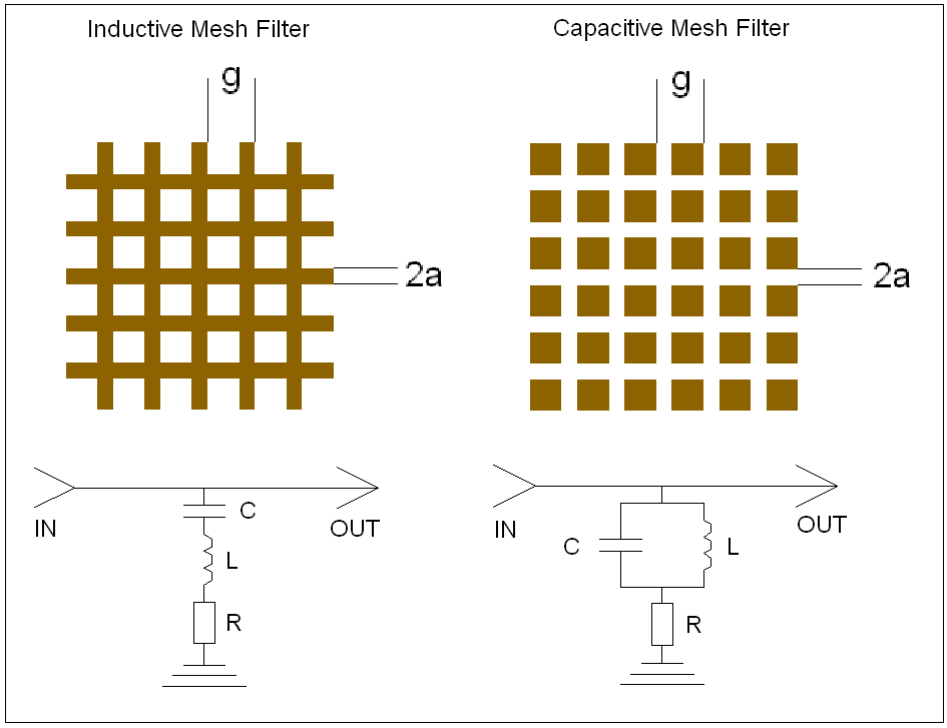

Figure 5: Layout of mesh filters.

4.2 Mesh Filters

The layouts of the inductive and capacitive mesh filters are shown in figure 5. The capacitive mesh consists of a grid of metal squares while the inductive mesh represents the complementary structure. These filters will also behave as low- and high-pass filters but have the additional advantage that the transmittance through the filter is independent of the polarization of the source. To see why this is the case, imagine that a linearly polarized source strikes the filter at normal incidence. We can decompose the polarization vector in the basis formed by the axes of the filter grid. But because the mesh filter (unlike the strip grating filter) is symmetric under rotation through 90 degrees, both components of polarization will "see" the same grid geometry. This means that both components have the same transmission and reflection coefficients, and the overall transmission coefficient is therefore not a function of the polarization angle.

Now let's consider the capacitive mesh geometry. Notice that each square is an "island" in the sense that there are no paths for current to flow between squares, so an electron in a given square is confined to move in that square alone. This is similar to the capacitive strip grating geometry in which electrons are confined to remain in one strip, and the two indeed behave similarly. The above argument pertaining to capacitive strip filters applies here: high-frequency sources excite rapid oscillations between two charged states and have poor transmittance, low-frequency sources are not absorbed by the confined electrons and have high transmittance.

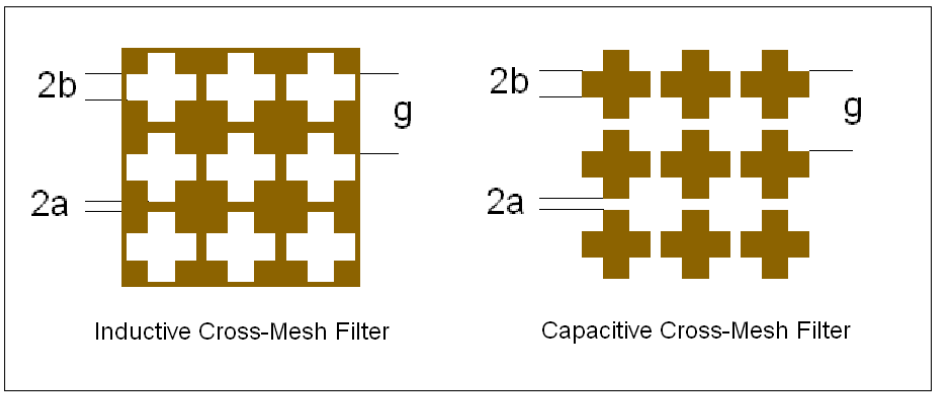

Figure 6: Layout of cross-mesh filters.

Now for the inductive mesh filter. In this geometry, electrons are not confined to move within a single square but have paths to flow all the way across the filter surface. This is similar to the inductive strip geometry, and the argument is again similar: low-frequency sources excite large-scale electron motion and have poor transmittance, high-frequency sources excite only small-scale "wiggling" of electrons and have high transmittance.

The equivalent circuits corresponding to capacitive and inductive mesh geometries are shown in figure 4. The impedances of the two circuits were determined empirically to be [8]:

$$X(f)_{ind} = -(w_0^{'} \ln \csc \frac{\pi a}{g})(\frac{gf}{cw_0^{'}} - \frac{cw_0^{'}}{gf})^{-1} \tag{3}$$

$$X(f)_{cap} = \frac{2}{n_1^2 + n_2^2}(4w_0^{'} \ln \csc \frac{\pi a}{g})^{-1}(\frac{gf}{cw_0^{'}} - \frac{cw^{'0}}{gf}) \tag{4}$$

where $w_0^{'} = w_o\sqrt{\frac{2}{n_1^2+n_2^2}}$. The value of w_0 is close to unity but must be determined empirically.

4.3 Cross-Mesh Filters

The last filter geometry that we are interested in is the cross-mesh geometry shown in figure 6. These filters are similar to mesh filters except that the repeated grid element is a cross instead of a square. The same principles discussed in the preceding two sections apply to the cross-mesh geometry.

The dimensions of these crosses determine a resonant wavelength. The resonant wavelength has a transmission zero for capacitive cross-mesh filters and has full transmission for inductive cross-mesh filters. The formula for the resonant wavelength was determined empirically to be:

$$\lambda_r = 2.27g - 4a - 2b \tag{5}$$

For a capacitive filter the transmittance goes to one as we move away from the resonant frequency, for the inductive filter the transmittance goes to zero. We were unable to find the equivalent circuits corresponding to the cross-mesh geometry, but the admittances of the two filters are [2]:

$$Y(f)_{ind} = \frac{1}{a_1 - i\frac{gA_1}{\lambda_r \Omega(f)}} \tag{6}$$

$$Y(f)_{ind} = \frac{1}{a_1 + i\frac{gA_1}{\lambda_r \Omega(f)}} \tag{7}$$

where a_1 and A_1 are the metal loss parameter and bandwith parameter, respectively. The values of these two parameters were found empirically by a least-squares fit to be $a_1 = .0001$ and $A_1 = .53$. In other words, we modeled several filters in High-Frequency Structure Simulator (HFSS) and with matrix methods and chose the values of a_1 and A_1 which minimized the deviation.

We refer to the function $\Omega(f)$ as the normalized frequency which is equal to [3]:

$$\Omega(f) = \frac{\lambda_r f}{c} - \frac{c}{\lambda_r f} \tag{8}$$

5 Matrix Methods

We use matrix methods [4] to determine the transmittance and reflectance of a given filter. Each filter is represented by a scattering matrix which depends only on the impedance of its equivalent circuit. If we wish to analyze systems consisting of multiple filters we simply multiply their scattering matrices together to obtain the scattering matrix of the system.

We begin with figure 7 in which we see a diagram of a circuit element of characteristic impedance Y as well as incoming and outgoing waves on both sides of the filter. The wave amplitudes a_1 (the incident wave) and b_1 (the reflected wave) on the left hand side are related to the wave amplitudes a_2 (incident wave) and b_2 (transmitted wave) on the right hand side by the following matrix:

$$\begin{pmatrix} b_1 \\ a_1 \end{pmatrix} = \begin{pmatrix} S_{11} & S_{12} \\ S_{21} & S_{22} \end{pmatrix} \begin{pmatrix} a_2 \\ b_2 \end{pmatrix} \tag{9}$$

If we assume that a_2=0, the ratio of the reflected wave to the incoming wave is:

$$r = \frac{b_1}{a_1} = \frac{S_{12}}{S_{22}} \tag{10}$$

and the ratio of the transmitted wave to the incoming wave is:

$$t = \frac{b_2}{a_1} = \frac{1}{S_{22}} \tag{11}$$

Now all that remains is to find the elements S_{ij} and we can determine the transmission and reflection coefficients by taking the appropriate ratios of these elements. These matrix elements can be obtained by applying Kirchoff's laws

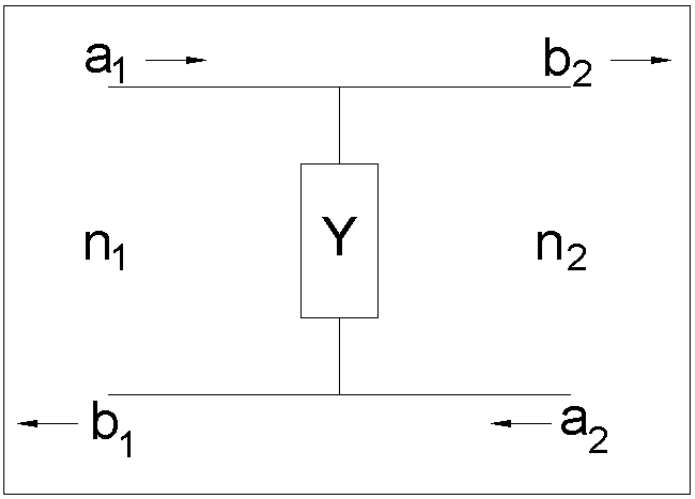

Figure 7:

to the circuit diagrammed in figure (), and the result for free-standing metal mesh is [4] [1]:

$$S = \begin{pmatrix} -\frac{Y(f)}{2} + 1 & -\frac{Y(f)}{2} \\ \frac{Y(f)}{2} & \frac{Y(f)}{2} + 1 \end{pmatrix} \tag{12}$$

Since the impedance Y is itself frequency-dependent, the transmittance and reflectance will also be functions of frequency. The above equations will therefore allow us to predict the transmittance through a given filter provided that we know the impedance of its equivalent circuit. The formula for the impedance of a given filter can be determined empirically.

At this point we have everything we need to analyze single-element, free-standing filters at normal incidence angle. We also would like to be able to analyze multiple-element filters, filters which lie on substrates, and filters which are struck by radiation at non-normal incidence. Each of these generalizations requires modifications to the above formulas.

5.1 Multiple Element Filters

The primary motivation for using matrix methods is that they are easily generalized to account for multiple elements in series. If a series of elements M_1, M_2, M_3, etc. have scattering matrices S_1, S_2, S_3, etc., we can find the scattering matrix corresponding to the multiple-element system by multiplying their individual matrices: S_{total}=...$S_3S_2S_1$. Note that matrix S_1 comes last in the above formula because it corresponds to the first element that the wave sees.

Before proceeding we must define the transport matrix [4] which tracks the phase change of the wave as it propagates between the individual filters:

[1] see Appendix B

$$T = \begin{pmatrix} e^{-\frac{2\pi i f d}{c}} & 0 \\ 0 & e^{\frac{2\pi i f d}{c}} \end{pmatrix} \tag{13}$$

where d is the distance between successive filters. Notice that the transport matrix simply introduces complex exponential factors and therefore does not affect the magnitude of the propagating waves. We can now find the scattering matrix corresponding to the full system consisting of multiple filter elements separated by spaces of distance d.

$$S_{total} = ...S_3 T_{32} S_2 T_{21} S_1 \tag{14}$$

The transmission and reflection coefficients of the system are obtained by using formulas 10 and 11 where the S_{ij} are now the elements of S_{total}.

5.2 Substrates

The above formulas apply only to free-standing metal meshes. Actual meshes are always grown on substrates, so we must be understand how the scattering matrices are changed when we have a metal mesh at the boundary of two media with indices of refraction n_1 and n_2

In this case, the scattering matrix of an individual filter becomes [4]:

$$S_{n_1 n_2} = \frac{1}{2n_1} \begin{pmatrix} -Y + (n_1 + n_2) & -Y + (n_1 - n_2) \\ Y + (n_1 - n_2) & Y + (n_1 + n_2) \end{pmatrix} \tag{15}$$

This result is obtained from transmission line theory by assuming that the circuit element sits at the junction of two transmission lines of characteristic admittances $Y_1 = n_1$ and $Y_2 = n_2$.

We must also alter the transport matrix to account for the index of refraction of the material between filters. When a wave passes from vacuum into a material of index of refraction n the wavelength is decreased by a factor n. To correctly track the phase change of the wave as it propagates through the material we must therefore take this effect into account in the transport matrix. This is accomplished by inserting a factor of n into the exponent of the transport matrix elements [4]:

$$T_n = \begin{pmatrix} e^{-\frac{2\pi i f d n}{c}} e^{-ad} & 0 \\ 0 & e^{\frac{2\pi i f d n}{c}} e^{-ad} \end{pmatrix} \tag{16}$$

We have also included a term e^{-ad} to account for the loss in the medium, where a is the loss constant with dimensions $length^{-1}$.

This wavelength-shrinking affect will also affect the resonant frequency of the filter. In general, for a filter between two materials of index of refraction n_1 and n_2 we have the following relation [3]:

$$\lambda_{res} \rightarrow \lambda_{res} \sqrt{\frac{n_1^2 + n_2^2}{2}} \tag{17}$$

which reduces correctly to the original form when $n_1 = n_2 = 1$. Notice that the effect is always to increase the resonant wavelength. Since the formula for the impedance of cross-mesh filters contains terms which are functions of λ_{res}, we must alter these impedance formulae accordingly.

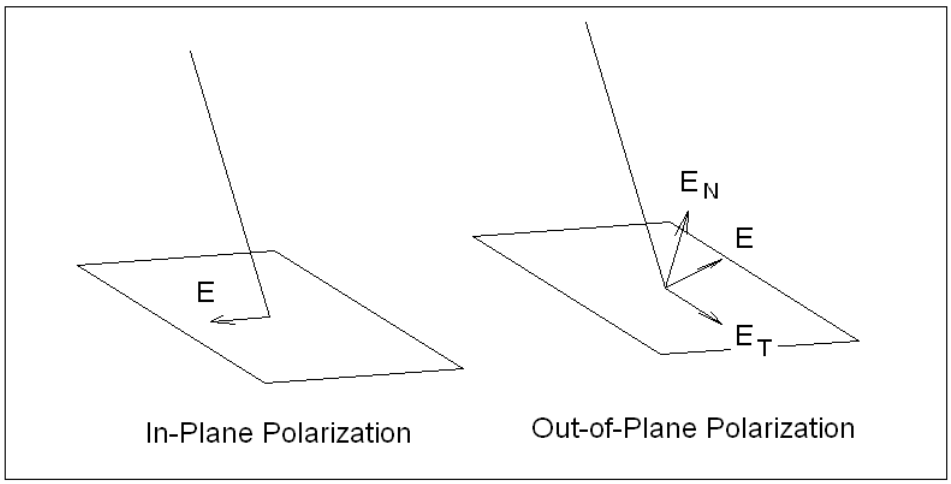

Figure 8: IP Polarization (left): Polarization vector lies in filter plane. OP Polarization (right): Polarization vector does not lie in filter plane and has components normal and tangent to the plane.

5.3 Non-Normal Incidence

If the wave strikes the filter plane at normal incidence the polarization vector will always lie in the plane. If we no longer assume normal incidence the E-field vector may or may not be in the filter plane depending on the polarization state of the source. In figure 8 we see two orthogonal polarization states, labeled in-plane (IP) and out-of-plane (OP). The polarization vector of the IP source is in the plane of the filter, while the polarization vector of the OP source has components normal and tangent to the surface. The normal component of the E-field cannot induce surface currents because the electrons are constrained to move in only two dimensions. This means that the normal component will not be able to transfer energy to the electrons and will therefore be fully transmitted. This means that the reflection and transmission coefficients of the IP and OP states will be different and we must track the coefficients of each polarization state individually. To do so we must understand how the impedance is altered for the two polarization states when the incidence angle is non-normal. We find that if a wave strikes the filter at some angle θ, the impedance of the OP state is multiplied by the cosine of that angle while the impedance of the IP state is divided by the cosine of the incidence angle [1]:

$$Y_{OP} = Y \cos\theta \tag{18}$$

$$Y_{IP} = \frac{Y}{\cos\theta} \tag{19}$$

The derivation of these two relations comes from decomposing the incident wave into waveguide modes and using waveguide theory to determine effective impedance [1].

Now we expand our scattering matrix to a 4x4 matrix which includes 4 2x2 sub-matrices. The diagonal sub-matrices represent the scattering matrices for

the two polarization states while the off-diagonal sub-matrices are null spaces:

$$S_{n_1 n_2} = \frac{1}{2n_1} \begin{pmatrix} -Y_{OP} + (n_1 + n_2) & -Y_{OP} + (n_1 - n_2) & 0 & 0 \\ Y_{OP} + (n_1 - n_2) & Y_{OP} + (n_1 + n_2) & 0 & 0 \\ 0 & 0 & -Y_{IP} + (n_1 + n_2) & -Y_{IP} + (n_1 - n_2) \\ 0 & 0 & Y_{IP} + (n_1 - n_2) & Y_{IP} + (n_1 + n_2) \end{pmatrix} \tag{20}$$

where Y_{OP} and Y_{IP} are determined by equations 18 and 19.

As before, the transmission coefficient is determined by taking the reciprocal of the (2,2) element of the relevant scattering sub-matrix. This time, however, we have two transmission coefficients, one corresponding to the OP state and the other to the OP state. The OP transmission coefficient is determined by taking the reciprocal of the (2,2) element while the IP transmission coefficient is determined by taking the reciprocal of the (4,4) element. The overall transmission coefficient of the source will be a linear combination of the coefficients corresponding to the two polarization states:

$$T_{total} = \sin^2 \theta_p T_{OP} + \cos^2 \theta_p T_{IP} \tag{21}$$

where θ_p is the polarization angle.

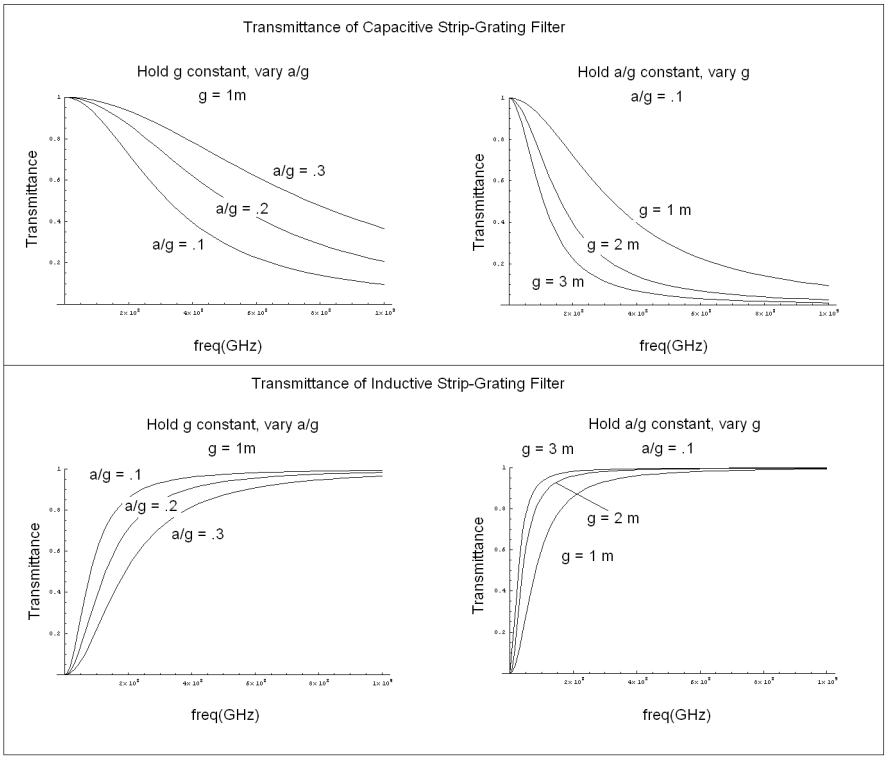

Figure 9:

6 Appendix A: Effect of Varying Grid Parameters

6.1 Strip Grating Filters

The steepness of the transmission curves for strip grating filters is a function of the ratio a/g as well as the grid spacing parameter g. Holding g constant and increasing the ration a/g makes the transmission drop more slowly. Holding a/g constant and increasing g makes the transmission drop more quickly.

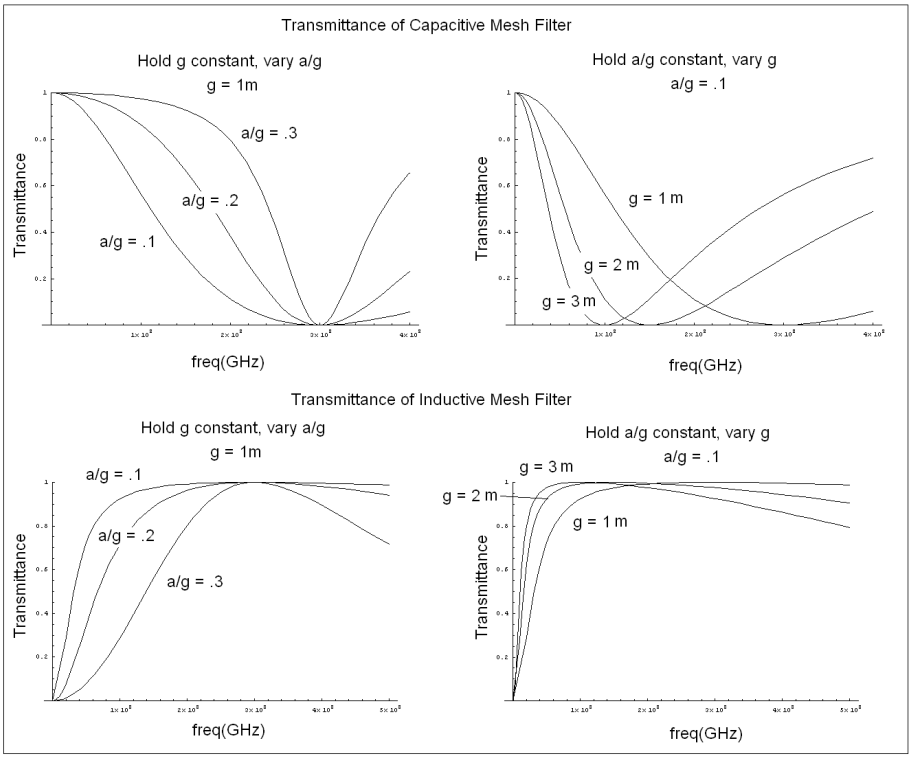

Figure 10:

6.2 Mesh Filters

The capacitive mesh filter has a transmission zero at frequency $f = \frac{c}{g}$. At frequencies above this critical frequency the transmission begins to rise steadily. The steepness of the curve depends on the ratio a/g, with a higher ratio leading to a steeper curve.

The inductive mesh filter has full transmission at frequency $f = \frac{c}{g}$, and the transmission begins to drop above this frequency. The steepness of the curve is again determined by the ratio a/g.

6.3 Cross-Mesh Filters

We find the following relations to hold (see figure 11):

Increasing the length of the crosses reduces the resonant frequency. Increasing the width of the crosses increases the bandwidth and increases the resonant frequency slightly. Increasing the substrate thickness decreases the resonant frequency slightly. Rounding the corners of the crosses increases the resonant frequency. Increasing the center-to-center spacing of the crosses decreases the bandwidth.

7 Appendix B: Derivation of Cascading Matrix

Given the diagram in figure 12, we wish to find the cascading matrix which satisfies:

$$\begin{pmatrix} b_1 \\ a_1 \end{pmatrix} = \begin{pmatrix} S_{11} & S_{12} \\ S_{21} & S_{22} \end{pmatrix} \begin{pmatrix} a_2 \\ b_2 \end{pmatrix} \tag{22}$$

In other words, we wish to find the amplitude coefficients a_1 and b_1 on the left hand side of the filter in terms of a_2 and b_2, the amplitude coefficients on the right hand side. To do so, we apply Kirchoff's current law and Ohm's law to the system diagrammed in the figure.

First of all, we need Ohm's law in a slightly altered form:

$$I = VY \tag{23}$$

where I is current, V is voltage and Y is admittance. We interpret the amplitude coefficients as voltages and the indices of refraction as admittances; in other words $Y_1 = n_1$ and $Y_2 = n_2$. This tells us that the current is equal to the amplitude coefficient times the index of refraction, as shown in the figure.

Now apply Kirchoff's current law to the two junctions where the transmission lines intersect the load element Y. This gives $I_1 = a_1 n_1 - b_2 n_2$ and $I_2 = b_1 n_1 - a_2 n_2$. Now we equate the voltage drop across the load element Y with the current across the load divided by the admittance:

$$b_2 - a_2 = V_y = \frac{I_Y}{Y} = \frac{I_1 - I_2}{Y} \tag{24}$$

Rearranging and plugging in for I_1 and I_2 gives:

$$Yb_2 - Ya_2 = a_1 n_1 - b_2 n_2 - a_2 n_2 + b_1 n_1 \tag{25}$$

which gives...

$$a_1 n_1 + b_1 n_1 = (-Y + n_2)a_2 + (Y + n_2)b_2 \tag{26}$$

Also, we know that the voltage drop on the left hand side is equal to the voltage drop on the right hand side:

$$a_1 - b_1 = b_2 - a_2 \rightarrow a_1 n_1 - b_1 n_1 = b_2 n_1 - a_2 n_1 \tag{27}$$

Adding and subtracting equations 18 and 19 gives:

$$2b_1 n_1 = [-Y + (n_1 + n_2)]a_2 + [Y + (n_2 - n_1)]b_2 \tag{28}$$

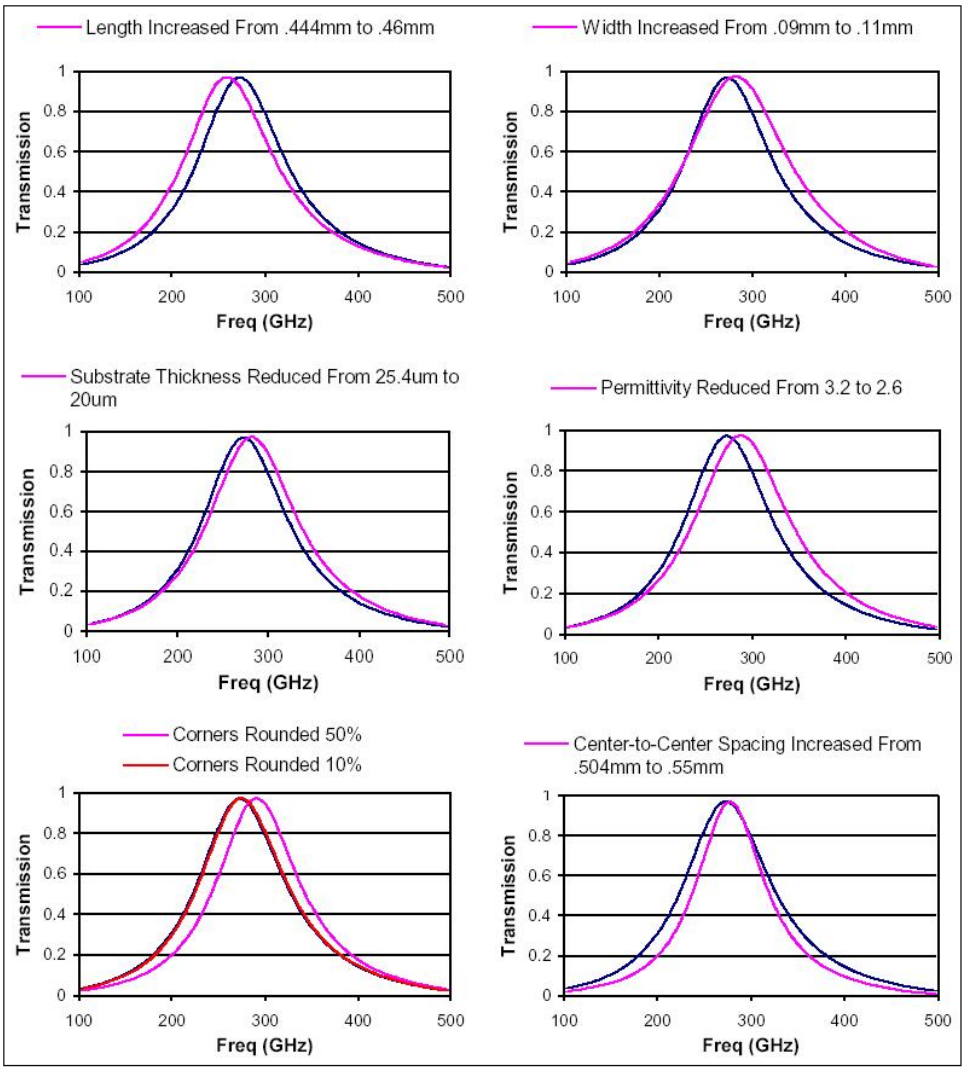
Length Increased From .444mm to .46mm
Width Increased From .09mm to .11mm
Substrate Thickness Reduced From 25.4um to 20um
Permittivity Reduced From 3.2 to 2.6
Corners Rounded 50%
Corners Rounded 10%
Center-to-Center Spacing Increased From .504mm to .55mm
Transmission
Freq (GHz)
0
0.2
0.4
0.6
0.8
1
100
200
300
400
500

Figure 11:

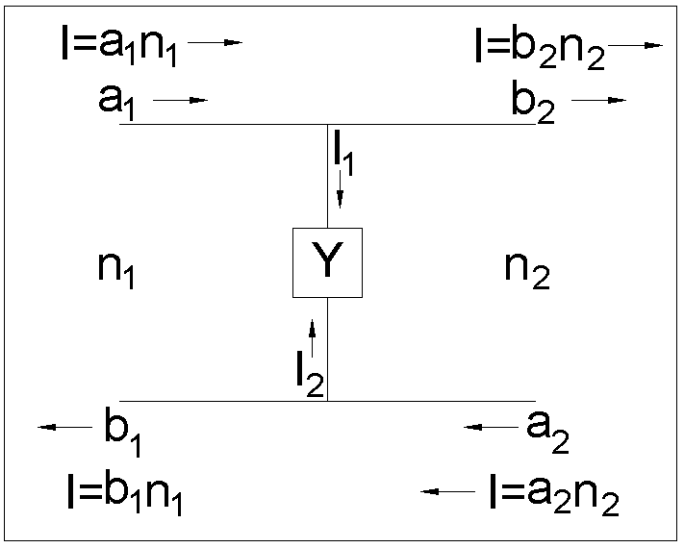

Figure 12:

$$2a_1n_1 = [-Y + (n_2 - n_1)]a_2 + [Y + (n_1 + n_2)]b_2 \tag{29}$$

This is almost the correct form of the cascading matrix except that the (1,2) and (2,1) elements are off by a factor of -1. The (1,2) element gives b_1 in terms of b_2, and the (2,1) elements gives a_1 in terms of a_2. But notice that the current corresponding to a_1 flows in the opposite direction of the current corresponding to a_2; likewise for b_1 and b_2. We must multiply by -1 those elements which give one current in terms of another which flows in the opposite direction, giving the correct form of the cascading matrix:

$$S_{n_1n_2} = \frac{1}{2n_1}\begin{pmatrix} -Y + (n_1 + n_2) & -Y + (n_1 - n_2) \\ Y + (n_1 - n_2) & Y + (n_1 + n_2) \end{pmatrix} \tag{30}$$

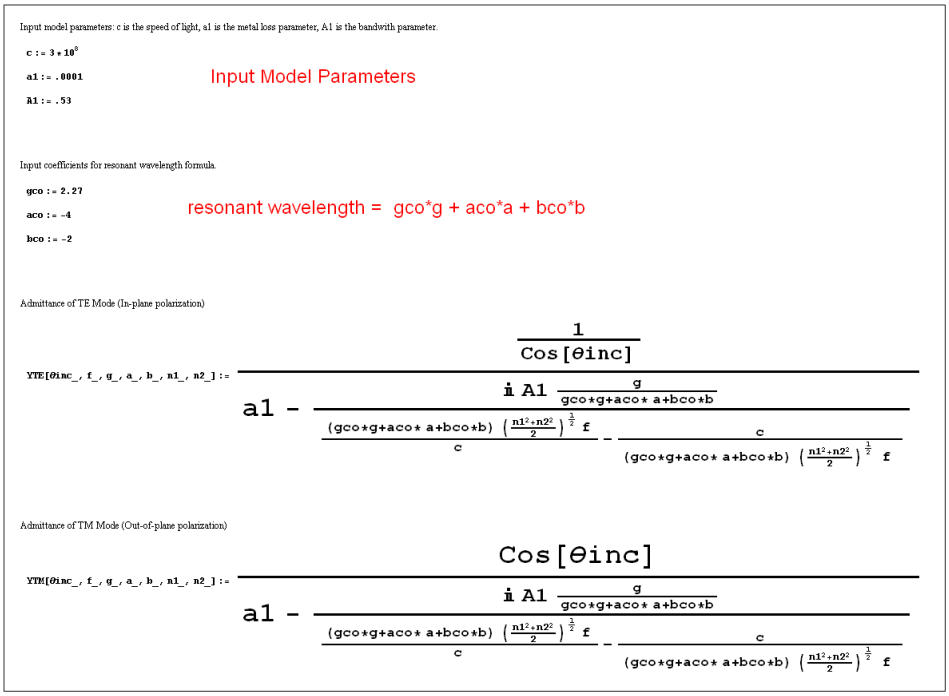

Figure 13:

8 How to Use the Mathematica File

The mathematica file can be found in MyDocuments/Ben's Filter Stuff/matrix method nonnormal.nb on the Inspiron 2400 Dell computer.

The grid parameters are to be entered into the boxes in blue, everything else may remain unaltered.

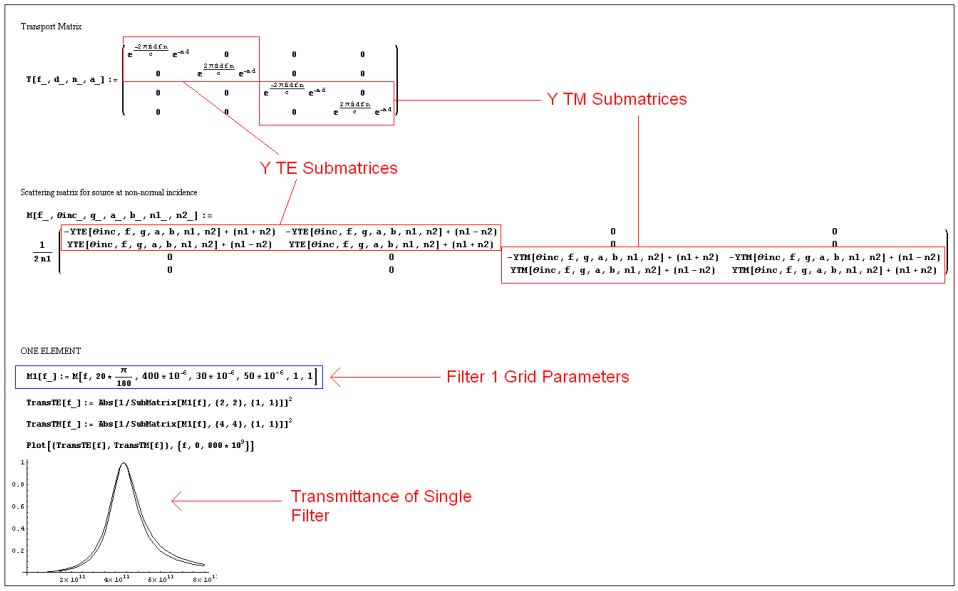

Figure 14:

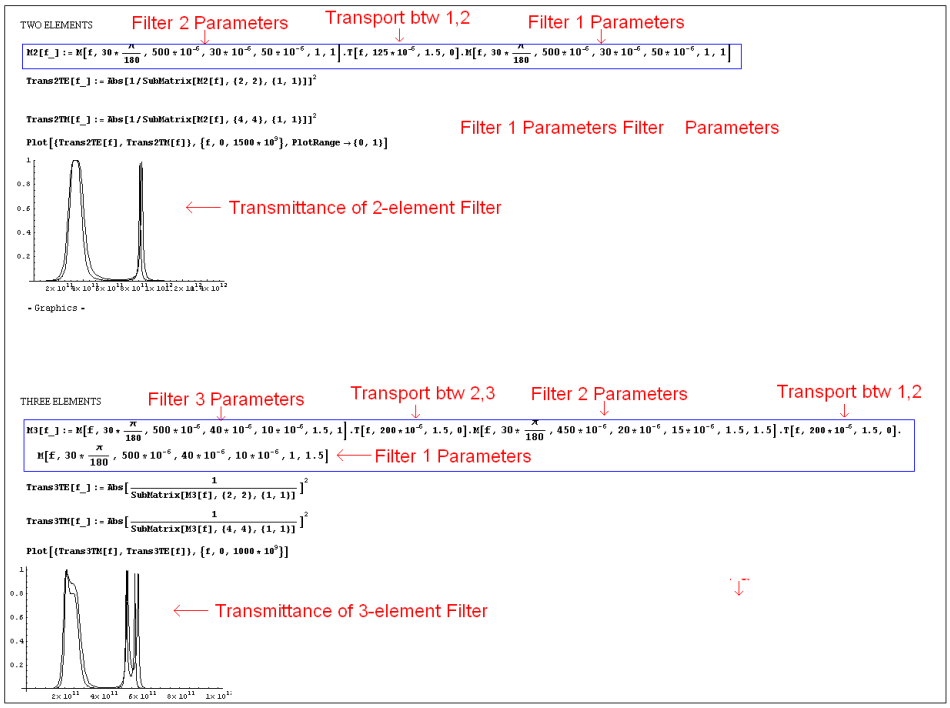

Figure 15: